Article

Effects of Climate Events on the Trophic Status of an Amazonian Estuary

Marcela Cunha Monteiro [1], **Luci Cajueiro Carneiro Perreira** [2,*] and **Rauquírio Marinho da Costa** [2]

1 Campus Tomé-Açu, Universidade Federal Rural da Amazônia, Rod. PA 140, 2428-4822, Tomé-Açu 68680-000, PA, Brazil; marcela.monteiro@ufra.edu.br
2 Instituto de Estudos Costeiros, Campus de Bragança, Universidade Federal do Pará, Alameda Leandro Ribeiro sn, Aldeia, Bragança 68600-000, PA, Brazil; raucosta@ufpa.br
* Correspondence: cajueiro@ufpa.br

Abstract: In recent years, climate events such as Drought, El Niño, and La Niña have become increasingly frequent and more intense. Oceanographic monitoring was used to collect hydrological data in the middle and lower sectors of the Caeté estuary in different years. Negative rainfall anomalies of up to 45% were recorded during periods marked by drought and El Niño events, which make the water in the Caeté estuary more saline and alkaline. During these events, the retention of dissolved inorganic nutrients in the middle sector appears to support increased eutrophication and more productive waters, whereas moderate eutrophication and lower productivity were observed in the lower sector. During La Niña events, by contrast, positive rainfall anomalies may reach 60%, resulting in more oxygenated water in the estuary. In addition, the lower sector tends to be more eutrophic during periods of high rainfall and freshwater discharge, as observed in this study during a La Niña event. The paucity of data on the effects of extreme climate events in Amazonian environments means that the findings of the present study may provide a useful model for the assessment of the effects of these events on other natural environments in the Amazon region.

Keywords: rainfall anomalies; hydrology; eutrophication

1. Introduction

Estuaries are considered to be the most biologically productive systems on Earth [1], with a mean primary production of 1500 g m^{-2} per year (dry matter), in comparison with only 125 g m^{-2} per year for the open ocean, 360 g m^{-2} per year for the waters of continental shelves, 400 g m^{-2} per year for lakes and streams, and 650 g m^{-2} per year for cultivated land [2]. Given their productivity, estuaries provide important feeding, spawning, and nursery areas for many migratory species found in both marine and freshwater environments [3,4].

Recent studies have shown that climate events such as the drought and the El Niño Southern Oscillation (ENSO) may affect these environments directly through anomalies in rainfall levels [5,6], which may result in a reduction in freshwater discharge, affecting both water quality and ecosystem goods and services [7]. ENSO is a climate pattern involving changes in the temperature of the waters in the central and eastern tropical Pacific Ocean, normally from 1 °C to 3 °C compared to normal conditions. The warm and cool patterns affect rainfall distribution in the tropics, and the El Niño and La Niña events are the extreme phases of the ENSO.

In estuaries, the principal changes can be observed in the availability and consumption of dissolved nutrients and organic matter, as well as in the occurrence of oscillations in the physical–chemical properties of the water and ecosystem structure and function [8]. These processes may result in variations in the trophic status and salinity of the estuary, as observed at a number of locations worldwide [5,9]. In the Amazon region, drought events make estuarine waters more saline and result in a reduction in dissolved nutrient

and chlorophyll *a* concentrations [6,10–12], whereas during periods of abnormally high rainfall, salinity declines and the water becomes richer in dissolved inorganic nutrients and phytoplankton biomass [13,14].

The annual variability in the climate of the Amazon region is controlled mainly by large-scale circulation patterns, including the displacement of the Inter-Tropical Convergence Zone (ITCZ). In the first half of the year, the ITCZ shifts to the Southern Hemisphere, triggering the formation of intense convective currents, which cause heavy rainfall (up to 90% of the annual total) and decreasing winds in this coastal region. During the second half of the year, the ITCZ shifts to the Northern Hemisphere, to about 10° north, causing rainfall to decline in the Brazilian Amazon Coastal Zone [15].

Inter-annual variations in rainfall levels in the Amazon region are closely linked to low-frequency, large-scale oceanic and atmospheric phenomena occurring over the Pacific (El Niño Southern Oscillation-ENSO) and Atlantic (North Atlantic Oscillation-NAO and Multidecadal Atlantic Oscillation-AMO) oceans [16,17]. The anomalous warming of the surface waters of these oceans has been associated with a reduction in rainfall levels, whereas anomalous cooling is associated with an increase in rainfall [18–22]. In this context, severe floods were recorded in the Amazon region in 1954, 1989, 1999, 2009, 2011, and 2012 [23–25]. A number of severe droughts have also been recorded in the region, with the first event being documented in 1911–1912 [26–30].

The Amazon drought of 2010 was one of the most severe episodes recorded in this region and was associated with some of the highest Sea Surface Temperatures (SSTs) ever recorded in the tropical Atlantic, coinciding with an El Niño event [21,23]. In 2012–2013, with high-pressure zones dominating the South Atlantic, anomalously cold southern waters migrated northward and contributed to a decline in rainfall levels in northeastern Brazil [31], a phenomenon that subsequently extended to the country's northern (Amazon) coast.

In this context, the main aim of the present study is to analyze the influence of interannual climate forcing, such as drought and ENSO events, on the water quality of an Amazonian estuary, the Caeté. The water quality in the Caeté estuary is determined primarily by the organic material and leaf litter deposited by the mangrove forests that surround the estuary [32], as well as the discharge of sewage and other untreated effluents from local settlements [33]. While the Caeté estuary is one of the best-studied bodies of water in the region, few studies have focused specifically on the effects of extreme climate events on its hydrological dynamics. In fact, this study is of great relevance because it shows physical and chemical data involving various climatic events, making it a pioneer for the sector under study. Given this, the principal question investigated in the present study is: How do anomalous climate events (Drought, El Niño, and La Niña) affect the trophic status of an Amazonian estuary? It is also hoped that the Caeté estuary can provide a useful model for the assessment of the effects of extreme climate events on the water quality of similar estuarine environments in the Amazon region, which may be affected by global climate change.

2. Study Area

The Caeté estuary (Figure 1) is located in northeastern Pará, about 150 km southeast of the mouth of the Amazon River, and forms the lower portion of the Caeté basin. This estuary is set within one of the world's largest continuous tracts of mangrove forest, which covers an area of 8900 km^2. The basin of the Caeté estuary has an area of 220 km^2 [34], of which approximately 180 km^2 is covered by mangrove forest [35]. This forest is flooded fortnightly, during the spring tides, and plays an important role in the nutrient profile of the adjacent coastal waters [36].
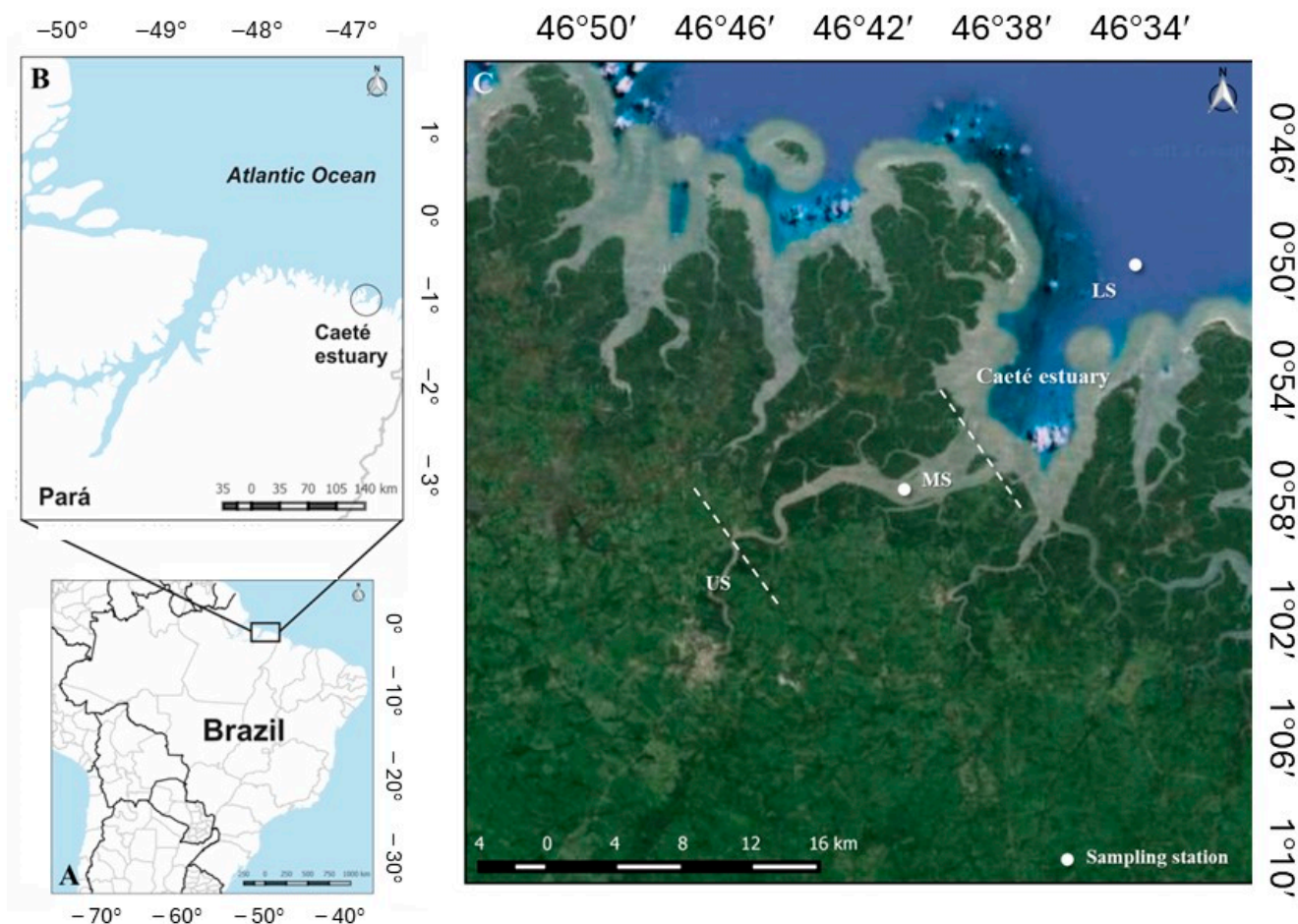
Figure 1. Location of study area on the northern coast of Brazil (**A**,**B**), showing the Caeté estuary (**C**) and the upper (US), middle (MS), and lower (LS) sectors of the estuary.

Based on a 39-year data series, the total annual rainfall in the study area ranges between 1400 and 4100 mm (Figure 2). In the study region, more than 80% of the total annual precipitation falls during the first half of the year, between January and July (the rainy season), when monthly rainfall exceeds 100 mm. The dry season is typically between August and December and normally accounts for less than 20% of total annual rainfall.

The Caeté River and its tributaries are the main source of freshwater discharge into the Caeté estuary. Based on a 15-year data series, the mean annual freshwater discharge of the Caeté ranges between 23.9 m^3 s^{-1} and 59.7 m^3 s^{-1} (Figure 2). In a typical year, around 70% of the total annual discharge is recorded during the rainy season, peaking in March, April, and May. By contrast, October, November, and December are the driest months.

The Caeté estuary is characterized by high levels of hydrodynamic energy. Local tides are semidiurnal and asymmetric, ranging between 2 m and 4 m during the neap tides and from 4 m to 6 m during the spring tides. Tidal current speeds are higher during spring tides and also present a seasonal pattern. During the rainy season, the ebb flow is more pronounced, peaking at around 1.2 m s^{-1} in the middle sector of the estuary and 1.5 m s^{-1} in the lower sector. During the dry season, the influence of marine forces increases and fluvial discharge decreases, contributing to stronger flood tide currents of around 1.5 m s^{-1} and 2.0 m s^{-1} in the middle and lower sectors, respectively. During neap tides, current speeds usually oscillate between 0.6 m s^{-1} and 0.7 m s^{-1} in both dry and rainy seasons in all sectors monitored (Figure 3). The maximum tidal prism recorded during neap tides was 72 × 10^6 m^3 [33,37].
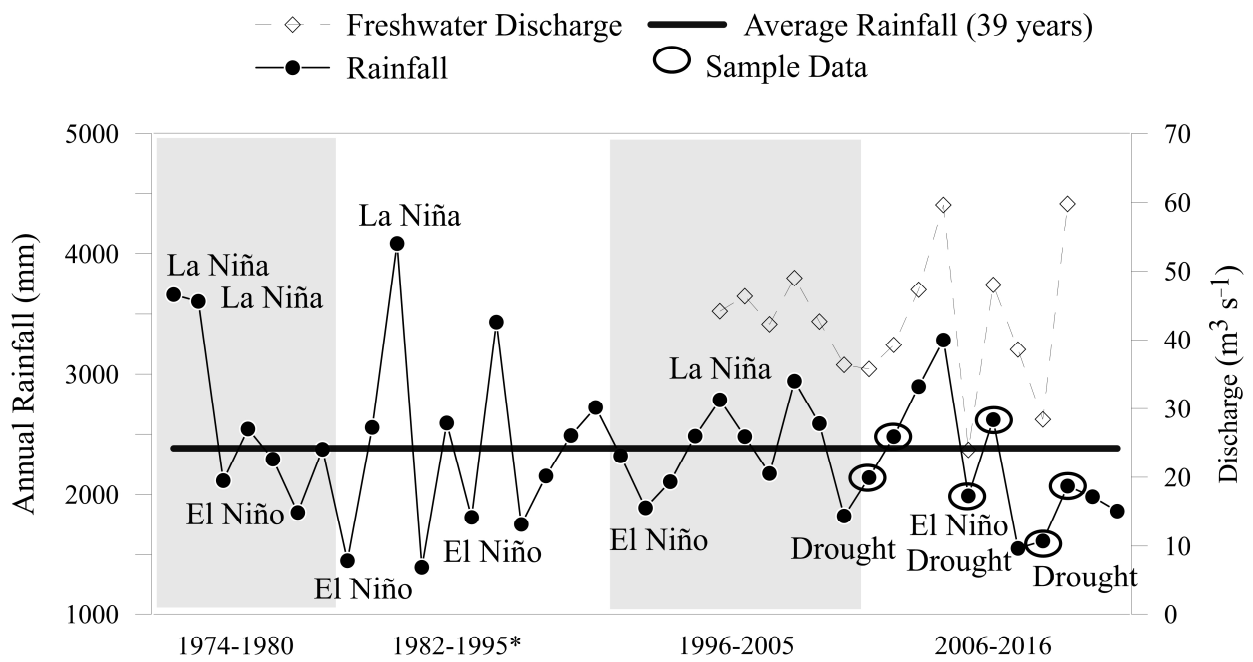
Figure 2. Annual rainfall in the Bragança region is based on a 39-year series of meteorological data. Source: INMET. * There are no data for 1981 or 1983.
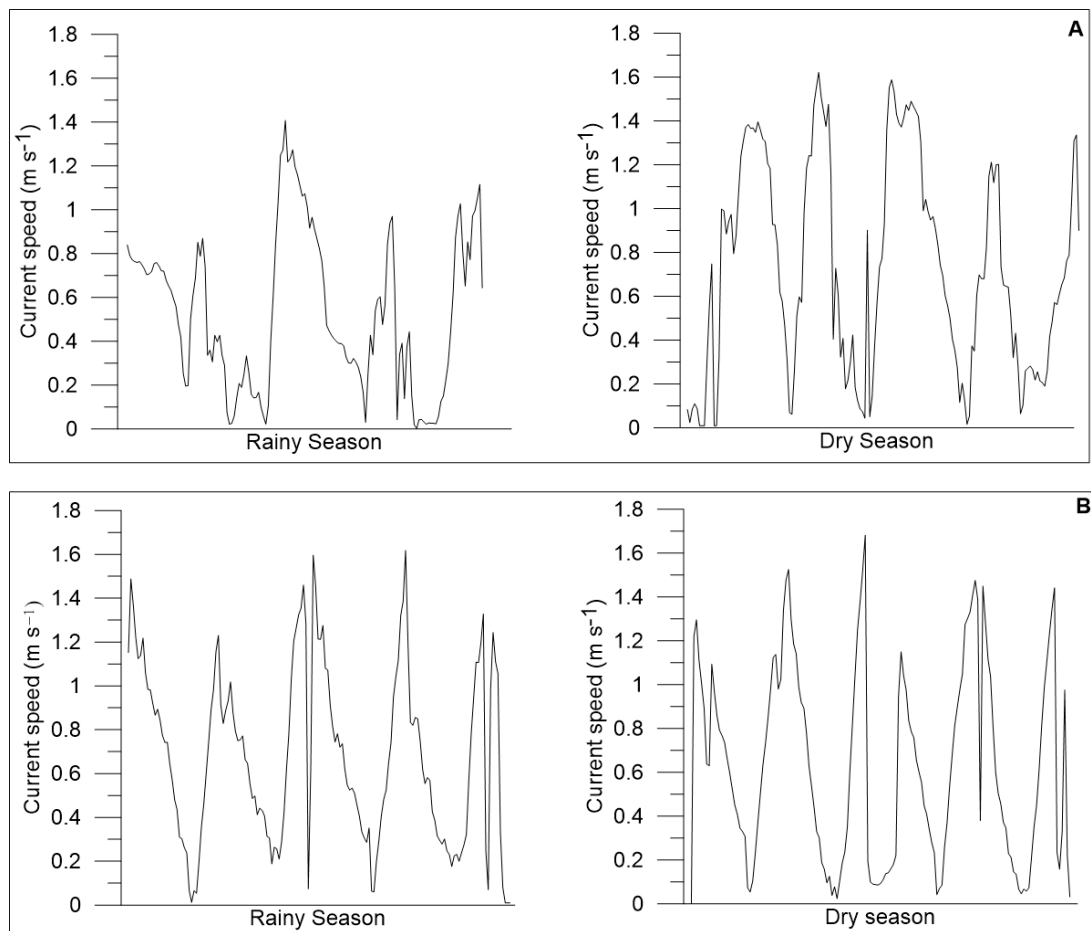

Figure 3. Current velocity in the Caeté estuary during the spring tide in the rainy and dry seasons in the middle (**A**) and lower (**B**) sectors.

The basin of the Caeté estuary has approximately 80,800 inhabitants [38], the majority (90%) of whom are residents in the town of Bragança, on the margins of either the Caeté estuary or the Cereja River, which flows into the Caeté estuary. A number of smaller communities are found in the middle and lower sectors of the estuary, with a total population of approximately 8259 inhabitants [39].

The trophic status of the Caeté estuary is determined by the combined effects of the presence of the mangrove forest, rainfall levels, freshwater discharge, and physical and anthropogenic factors. These variables act together as an important regulator of water quality through the control of trophic and microbiological conditions [33,40,41].

3. Data and Methods

3.1. Methodology for Assessing Climate and Hydrological Conditions

To understand the functioning of the Caeté estuary, data were collected on rainfall and freshwater discharge levels, as well as spatial and temporal oscillations in physical–chemical variables during several years under both typical conditions and those forced by extreme climate events. Information on the occurrence of extreme climate events was obtained from the National Oceanic and Atmospheric Administration [42] and from regional studies [21,23–25,43].

The rainfall data were provided by the National Meteorological Institute (INMET), and records of the freshwater discharge of the Caeté River were obtained from the National Water Agency (ANA). The climate data were recorded for the 39-year period between 1974 and 2016 (except 1981 and 1983), while the hydrological data refer to the 15-year period between 2000 and 2014 and were obtained from the gauge station located approximately 30 km upstream from the middle sector of the Caeté Estuary.

Oceanographic monitoring was used to collect hydrological data at 1.0 m below the surface in the middle and lower sectors of the estuary during the rainy and dry seasons in different years under typical (April and June in 2006 and 2014, and September and October in 2011) and atypical conditions (El Niño: August, October, and December in 2006, and February in 2007; Drought: September and November in 2010; June, October, and December in 2013; La Niña: December 2010; January, March, May, and July in 2011).

Data were collected using CTDs equipped with sensors that measured salinity, pH, dissolved oxygen, and turbidity (RBR XR-420) at 10-s intervals for 5 min. Niskin bottles of 5 L (General Oceanics, Miami, FL, USA) were used to obtain water samples for the analysis of dissolved inorganic nutrients (nitrite, nitrate$^-$, ammonium, phosphate$^-$, and silicate) and chlorophyll *a* concentrations. A total of 80 water samples were collected during the flood–tidal cycle.

3.2. Methodology for Determining Physical and Chemical Indicators of Water Quality

In the laboratory, water samples were vacuum filtered using glass fiber filters (Whatman GF/F 0.7 μM, 47 mm), and nutrient and chlorophyll-a concentrations were analyzed. Chlorophyll-a (Chl-a) was extracted with a 90% acetone *v*/*v* solution, and its concentration was quantified spectrophotometrically (Thermo Scientific 220 Evolution UV–Vis, Waltham, MA, USA) according to the protocols of [44,45]. Dissolved nutrient concentrations were also determined by spectrophotometry using the methods of [46,47]. The reagents used were of high purity, usually over 95 percent, guaranteeing the reliability of the results.

The spectrophotometer used for the analyses of nutrients and the limits of detection (DLs) established were DL = 0.05 μM for nitrate, DL = 0.01 μM for nitrite, DL = 0.05 μM for ammonium, DL = 0.03 μM for orthophosphate, and DL = 0.02 mg m^{-3} for chlorophyll-a. It was calibrated with deionized water (mixed bed deionizer Q-380 M). To maintain quality control standards, the linearity of the chemical method ($R^2 > 0.998$) was established using individual calibration curves. These curves were constructed using standard solutions with known concentrations of the respective substances.

The trophic status of the estuary was determined using the TRIX index proposed by [48], where Chl *a* is the chlorophyll *a* concentration, $DO_2\%$ is the oxygen saturation rate,

DIN is the dissolved inorganic nitrogen concentration (nitrite + nitrate + ammonium), DIP is the concentration of dissolved inorganic phosphorus, and *k* and *m* are constants with values of 1.5 and 1.2, respectively.

$$\text{TRIX} = (\log_{10}[\text{Chl } a \times |DO_2\%| \times \text{DIN} \times \text{DIP}] + k)/m$$

The TRIX index provides scores of 0–10, which are assigned to four classes: (i) 0–4: low eutrophication and high water quality; (ii) >4–5: moderate eutrophication and good water quality; (iii) >5–6: high eutrophication and bad water quality; and (iv) >6–10: elevated eutrophication and poor water quality. As the area of the present study is a relatively undisturbed natural environment, the terms "poor" and "bad" water quality classes were not applied here.

3.3. Methodology of Statistical Data Processing

The physical and chemical data were analyzed spatiotemporally by sector (middle and lower estuaries), season (dry and rainy), and climate event (Drought, El Niño, and La Niña). The assumptions of data normality and the homogeneity of variances were evaluated using Lilliefors' test [49] and Bartlett's Chi-square [50], respectively. When the data were not normally distributed or the variance was not homogeneous, the data were *log* (*x* + 1) transformed to produce a near-normal or near-homogeneous distribution. Parametric tests (Student's *t*-test) were used to assess whether the hydrological parameters varied significantly by sector, season, or climate event. For data that remained non-normal or heterogeneous, even after transformation, the nonparametric Mann–Whitney *U* and Kruskal-Wallis *H* tests were applied. Environmental variables were also evaluated using a Spearman rank correlation analysis. A Principal Components Analysis (PCA) was used to verify the relationship between rainfall and hydrological parameters in both estuarine sectors under different climate events. All these analyses were run in STATISTICA 8, with a significance level of $p < 0.05$.

4. Results

4.1. Climatological Aspects

4.1.1. Typical Conditions

As described above, the rainfall recorded in April and June in 2006 and 2014 was typical of the expected rainy season conditions, and the precipitation recorded in September and October 2011 was also typical of the dry season. In the rainy season of 2006, the total rainfall between January and July 2006 was 2000 mm, corresponding to 90% of the total precipitation recorded this year. The rainfall recorded during the year was similar to the historical mean. The highest monthly rainfall (465 mm) was recorded in March 2006 (Figure 4A). The freshwater discharge of the Caeté River in 2006 was also typical of the historical mean, with an average of 53 m^3 s^{-1} in the rainy season, corresponding to 81% of the total annual discharge. The high rainfall levels recorded in February and March provoked a peak in the discharge (83 m^3 s^{-1}) in April (Figure 4A).

In the dry season of 2011, the total rainfall recorded between August and December was approximately 140 mm, corresponding to 5% of the annual total (Figure 4B). At the beginning of the dry season, monthly precipitation was around 70 mm, but at the end of the period, negligible values (less than 5 mm) were recorded. These low rainfall levels were reflected in reduced freshwater discharge. The mean discharge recorded in this period was 19 m^3 s^{-1}, with monthly levels of between 11 m^3 s^{-1} and 40 m^3 s^{-1} (Figure 4B).

In the rainy season of 2014, total rainfall was 2070 mm, similar to the historical mean, and once again, corresponded to approximately 90% of the total annual rainfall. A monthly rainfall of between 300 mm and 500 mm was recorded in February–May (Figure 4C), resulting in high freshwater discharge at a mean level of 60 m^3 s^{-1} and peaking at 97 m^3 s^{-1} in May, following the heavy rains of the preceding months (Figure 4C).
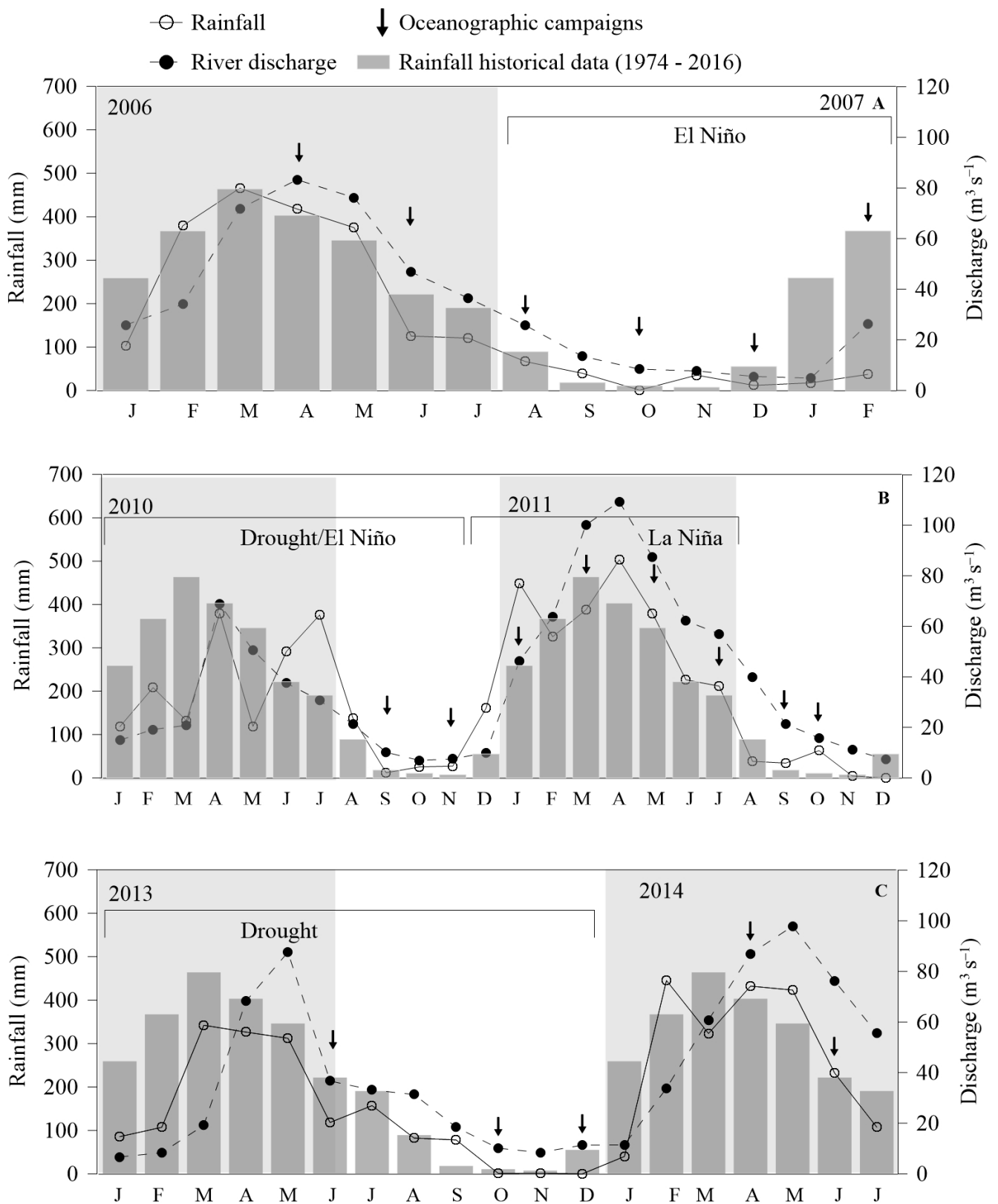
Figure 4. Monthly rainfall in Bragança and the freshwater discharge of the Caeté River during the oceanographic campaigns, 2006–2007 (**A**), 2010–2011 (**B**), 2013–2014 (**C**). The hatched gray areas represent the rainy season, and the arrows represent the months of collection.

4.1.2. Atypical Conditions

El Niño Event: Dry Season (2006) and Rainy Season (2007)

An El Niño event occurred between August 2006 and February 2007. Despite this, rainfall levels recorded during the dry season of 2006 were similar to the historical mean, at 153 mm, which corresponds to around 10% of the annual total (Figure 4A). The mean freshwater discharge was 12 m^3 s^{-1}, only slightly lower than expected for this season (Figure 4A). In this season, then, the effects of El Niño or drought events are less pronounced due to the prevailing conditions, i.e., low rainfall rates, primarily observed even in typical years. During the rainy season of 2007, however, the El Niño event appeared to have a clear impact on rainfall levels, given that only 57 mm was recorded in January and February, corresponding to 8% of the expected rainfall for this period (Figure 4A). The mean freshwater discharge was approximately 15 m^3 s^{-1}, 60% lower than expected for this period.

La Niña Event: Dry Season (2010) Rainy Season (2011)

The La Niña event began in December 2010 and persisted until July 2011. During the first month, rainfall was 100% higher than usual, reaching 160 mm. The total rainfall recorded during this event was approximately 2200 mm, 15% higher than that expected for this period. Monthly rainfall peaked at 503 mm in April. This increase in rainfall levels was associated with an increase of 30% in the freshwater discharge recorded during this period, which averaged around 75 m^3 s^{-1} (Figure 4B).

Drought Event: Dry Season (2010) and Rainy and Dry Seasons (2013)

A drought event was recorded in 2010. Despite this, during the second semester, when the oceanographic campaigns began, the rainfall rate was higher than expected due to the atypical pattern recorded in July and August, which resulted in a total rainfall of around 515 mm. However, the freshwater discharge did decline considerably, to 14 m^3 s^{-1}, reflecting the low rainfall rate recorded in the first semester, 40% lower than expected.

The next drought began in January 2012 and lasted until 2013, with a total annual rainfall of 1552 mm and 1612 mm, respectively. These are the lowest annual rainfall values recorded over the past 30 years and represent only 65% of the historical mean for the Bragança region. In June 2013, when the oceanographic campaign was conducted, total rainfall was only 118 mm, well below the value expected for this month (Figure 4C). Despite this drought event, the typical seasonal pattern was upheld, with 80% of the total annual rainfall being recorded during the rainy season. During the dry season, oceanographic campaigns were conducted in October and December, when rainfall was negligible, being less than 1 mm (Figure 4C).

The mean freshwater discharge of the Caeté River in 2013 was 28 m^3 s^{-1}, well below the historical mean of 40 m^3 s^{-1} (Figure 4C). This reflected the reduced total rainfall recorded this year. During the rainy season, the mean discharge was 37 m^3 s^{-1}, compared with 15 m^3 s^{-1} during the dry season.

4.2. Hydrological Aspects

Spatial and temporal variations in hydrological parameters and trophic status reflect the balance of the freshwater discharge and the incursion of marine water into the estuary. Here, the hydrological conditions recorded in the middle and lower sectors of the Caeté Estuary are presented for the different monitoring periods.

Overall, the highest salinity and pH values were recorded when rainfall reached its lowest levels, i.e., during the dry season, El Niño, and drought events. Salinity was thus negatively correlated with rainfall in both the middle ($r_s = -0.80$; $p < 0.05$) and lower sectors ($r_s = -0.60$; $p < 0.05$) of the estuary (Tables 1 and 2). In the case of the pH, a negative correlation with rainfall was recorded only in the middle sector ($r_s = -0.58$; $p < 0.05$, Table 1).

Table 1. Correlation matrix of water quality indicator values, rainfall, and salinity values in the middle sector.

	Salinity	pH	DO%	Nitrite	Nitrate	Ammonium	Ortophosphate	Silicate	Chlorophyll-a	Turbidity
Rainfall	−0.80 *	−0.58 *	0.10	−0.40	−0.38	0.03	−0.47 *	−0.42	0.13	0.00
Salinity	-	0.84	−0.14	0.45	0.17	−0.26	0.16	0.31	0.02	−0.28

* Significance level ($p < 0.05$).

Table 2. Correlation matrix of water quality indicator values, rainfall, and salinity values in the lower sector.

	Salinity	pH	DO%	Nitrite	Nitrate	Ammonium	Ortophosphate	Silicate	Chlorophyll-a	Turbidity
Rainfall	−0.60 *	−0.40	0.35	0.61 *	0.43	−0.08	−0.36	0.41	0.09	−0.50 *
Salinity	-	0.22	−0.26	−0.63 *	−0.57 *	−0.02	0.36	−0.52 *	0.24	0.40

* Significance level ($p < 0.05$).

During typical years, salinity in the middle sector is around 4 in the rainy season and 16 in the dry season. Under drought or El Niño conditions, however, the reduction in rainfall levels and freshwater discharge act synergistically, contributing to significantly more saline ($H = 15.1$; $p < 0.001$) and alkaline ($H = 14.6$; $p < 0.01$) waters. Salinity values of over 26 were recorded during both the rainy and the dry seasons. La Niña events had a less pronounced effect on salinity, however, which was little altered despite the reduction in rainfall levels (Figure 5). A similar pattern was observed in the lower sector (Figure 6).

In the middle sector of the estuary, the influence of the freshwater discharge of the Caeté River is more pronounced, resulting in salinity of 3–35 ($U = 68.0$; $p = 0.00$), pH lower than 7.8 ($U = 88.5$; $p = 0.00$), and dissolved oxygen saturation usually lower than 100% ($U = 85.0$; $p = 0.01$, Figure 5). The lower sector, in turn, was influenced more by the marine waters of the Atlantic Ocean, with salinity of 20–38, a predominantly alkaline pH (usually higher than 7.8), and dissolved oxygen saturation between 87 and 135% (Figure 6).

Turbidity was correlated negatively with rainfall ($r_s = -0.50$; $p < 0.05$, Table 2) in the lower sector, and a significant increase was observed in this sector during drought events ($F = 0.00$; $p < 0.001$). Drought events occur mainly during the dry season, when hydrodynamic energy is higher and supports the suspension of sediments in the water column. In the middle sector, where the influence of freshwater discharge is greater, values of 100–440 NTU were recorded (Figure 5). In the lower sector, turbidity was lower than 100 NTU (Figure 6).

High turbidity, as observed during drought events, restricts the penetration of light into the water column, leading to a reduction in the production of oxygen by phytoplankton and the exchange of gases with the atmosphere. An increment in oxygen saturation was observed during La Niña events in both the middle ($H = 12.8$; $p < 0.001$) and lower ($F = 51.1$; $p < 0.01$) sectors, probably due to the turbulence at the water surface caused by the more intense river flow. Dissolved oxygen concentrations were saturated primarily in the lower sector (Figures 5 and 6), where a negative correlation ($r_s = -0.6$, $p < 0.05$) was found with turbidity.

An increase in dissolved inorganic nutrient concentrations was observed in the middle sector in both the rainy and dry seasons of the negatively anomalous periods, characterized by reduced rainfall (<50 mm) and freshwater discharge (<36 m^3 s^{-1}), as observed during drought and El Niño events. During a typical rainy season, the concentration of nitrite was 0.4 μM, nitrate was 3.3 μM, ammonium was 1.9 μM, ortophosphate was 1.8 μM, and silicate was 33.0 μM. Under drought or El Niño conditions, by contrast, these values increased to 2.5 μM for nitrite, 9.2 μM for nitrate, 2.2 μM for ammonium, 2.2 μM for ortophosphate, and 150.0 μM for silicate. A similar pattern was observed during the dry season. By contrast, during the La Niña event, when rainfall (>250 mm) and freshwater discharge (>65 m^3 s^{-1}) were both higher, the concentrations of all inorganic nutrients, except nitrate, decreased.

The maximum observed concentrations were 0.2 μM for nitrite, 1.5 μM for ammonium, 0.4 μM for ortophosphate, and 94.6 μM for silicate (Figure 7).
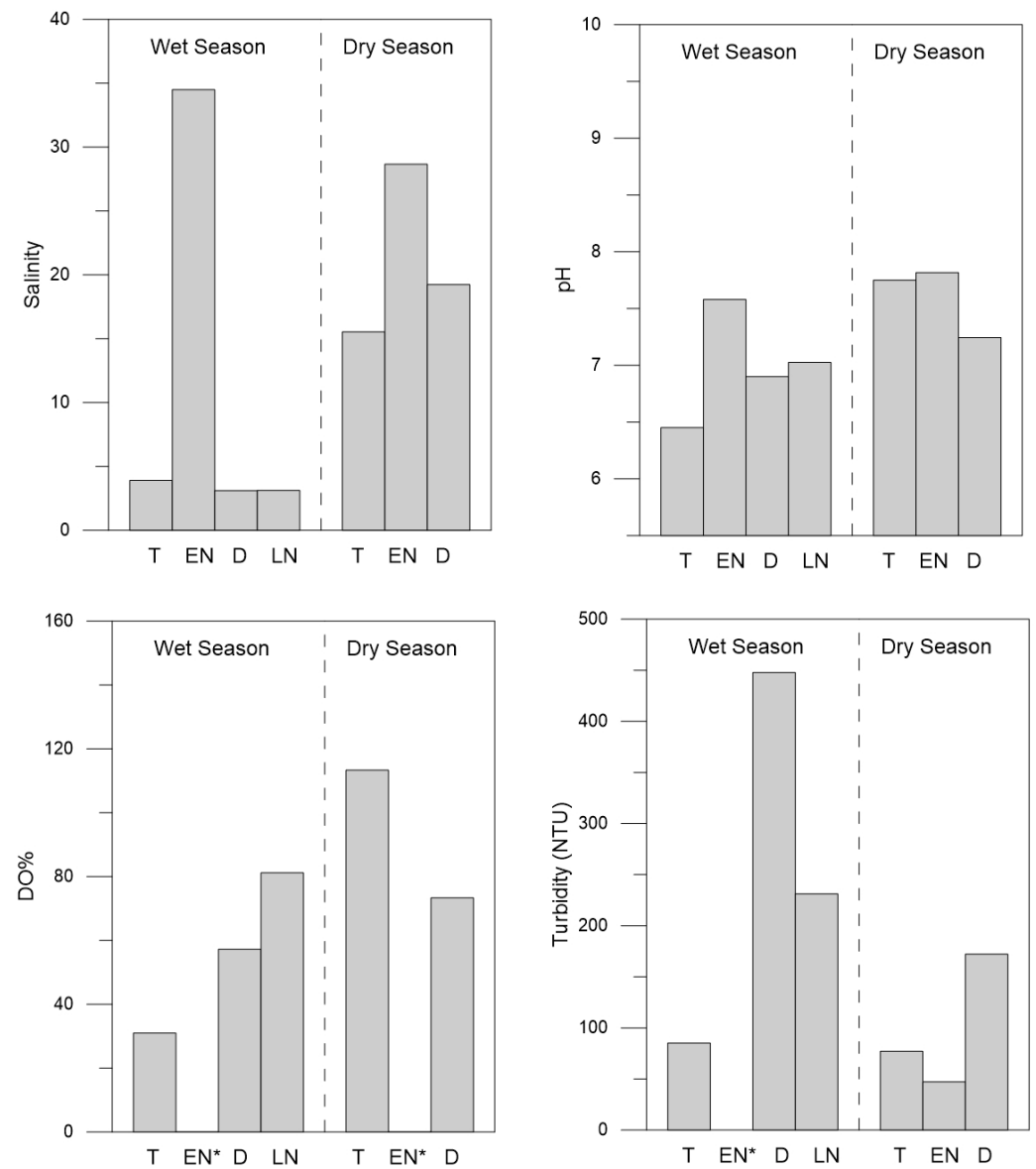

Figure 5. Salinity, pH, oxygen saturation, and turbidity were recorded in the middle sector of the Caeté estuary during typical (T) and atypical (EN: El Niño, D: Drought, and LN: La Niña) periods. (*) Not sampled.
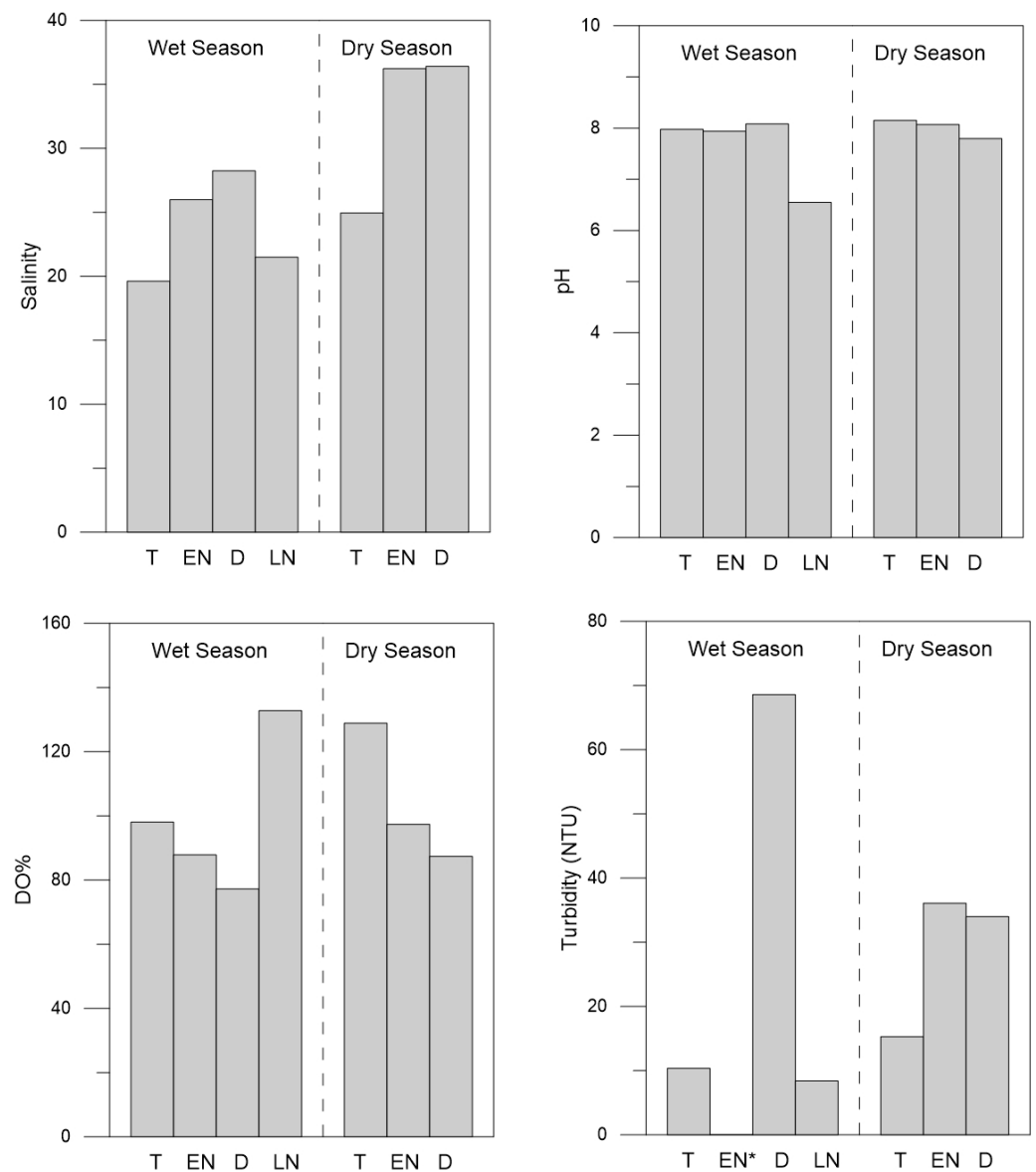
Figure 6. Salinity, pH, oxygen saturation, and turbidity were recorded in the lower sector of the Caeté estuary during typical (T) and atypical (EN: El Niño, D: Drought, and LN: La Niña) periods. (*) Not sampled.

The lower sector presented the exact opposite pattern, with low dissolved inorganic nutrient concentrations being recorded under drought and El Niño conditions. The maximum values recorded in this period were 0.2 μM for nitrite, 2.3 μM for nitrate, 2.1 μM for ammonium, 0.2 μM for ortophosphate, and 37.4 μM for silicate, whereas relatively high concentrations were recorded under La Niña conditions (except for ammonium), i.e., 1.0 μM for nitrite, 8.3 μM for nitrate, 0.4 μM for ortophosphate, and 85.0 μM for silicate (Figure 8). Freshwater discharge from the hydrographic basin is usually the main source of nutrients for adjacent coastal waters, which explains the positive correlation between the different dissolved nutrients observed in the lower sector (nitrite vs. nitrate: $r_s = 0.7$, $p < 0.05$; nitrate vs. silicate: $r_s = -0.4$, $p < 0.05$).
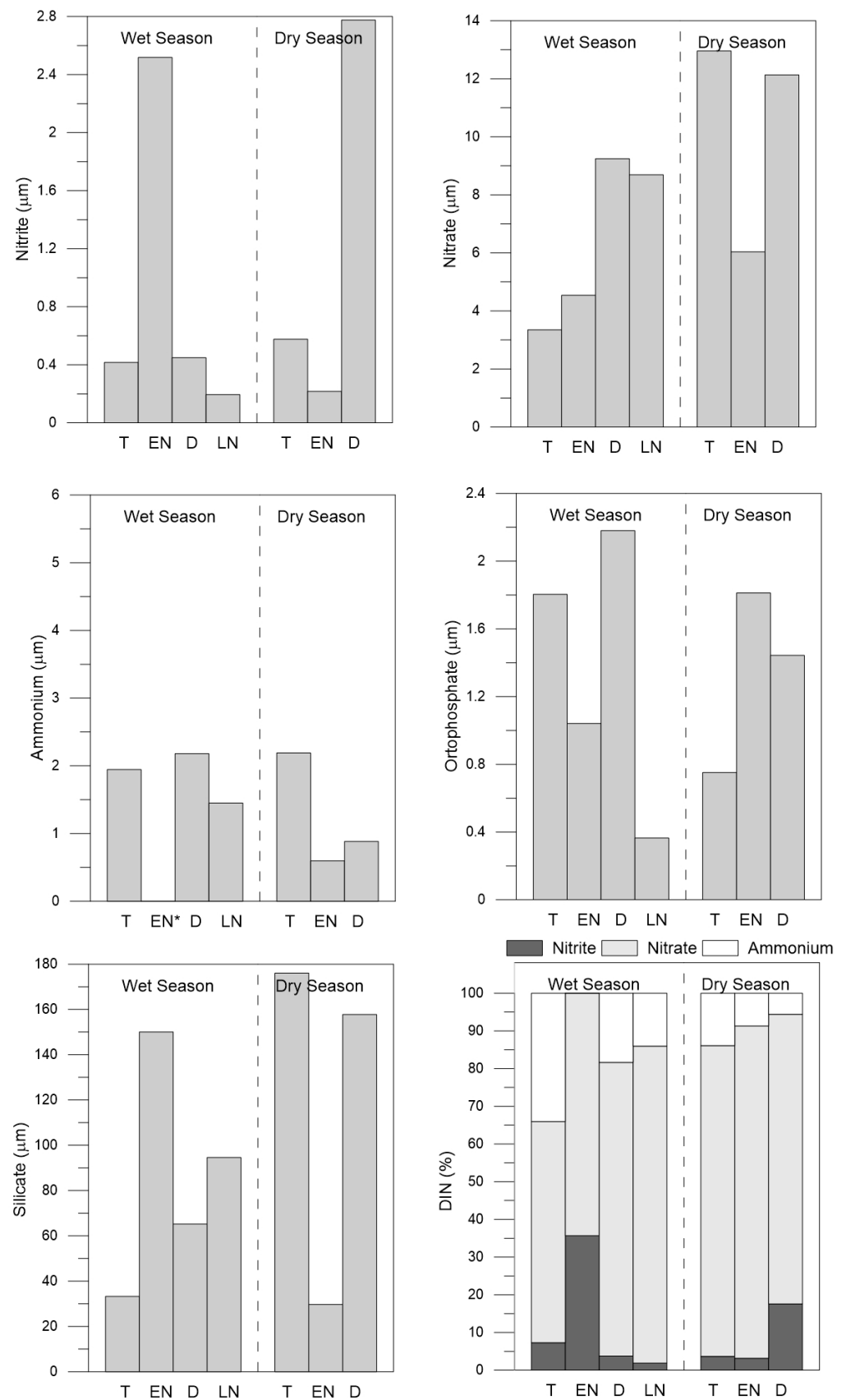
Figure 7. Dissolved nutrient concentrations were recorded in the middle sector of the Caeté estuary during typical (T) and atypical (EN: El Niño, D: Drought, and LN: La Niña) periods. (*) Not sampled.
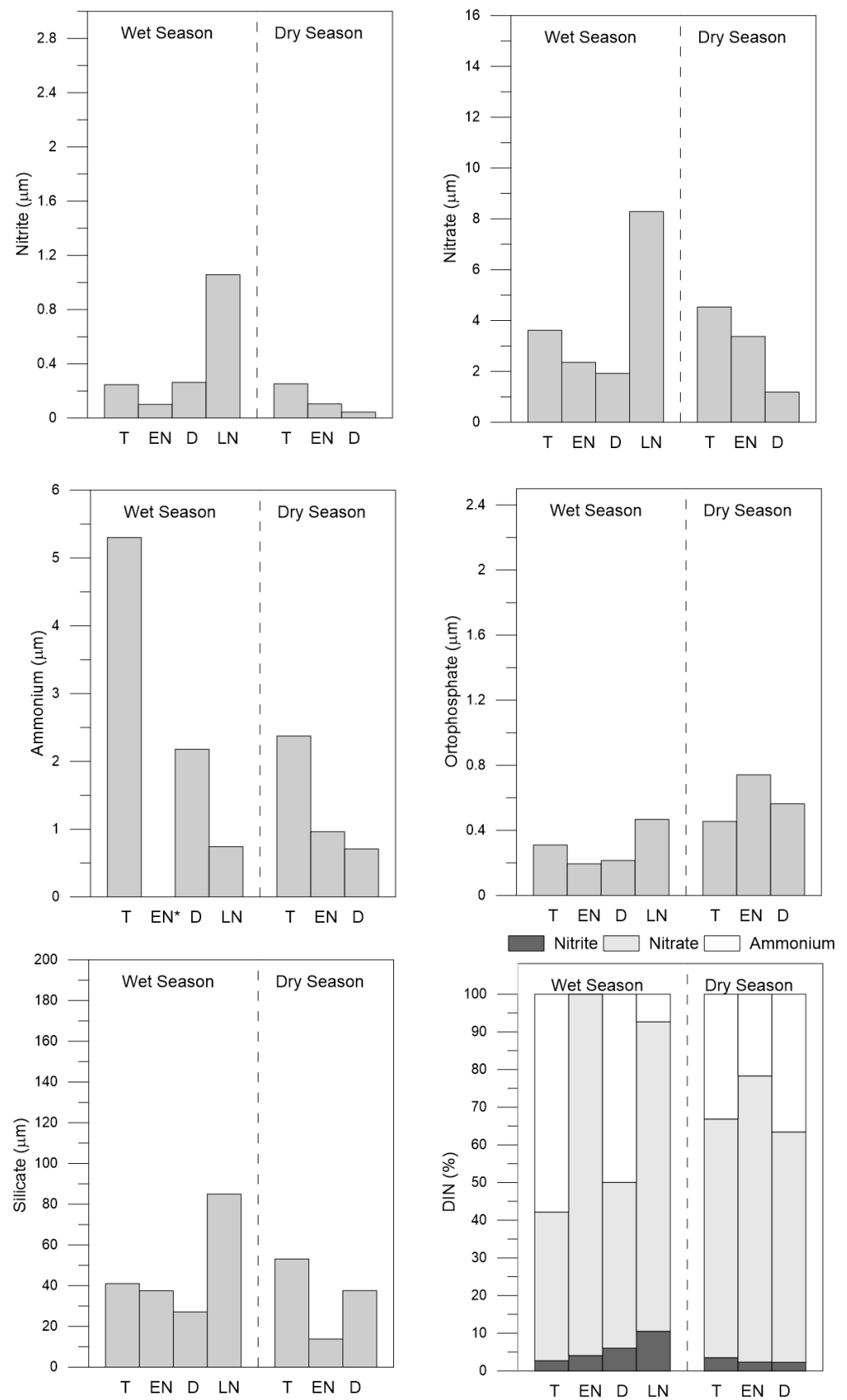
Figure 8. Dissolved nutrient concentrations were recorded in the lower sector of the Caeté estuary during typical (T) and atypical (EN: El Niño, D: Drought, and LN: La Niña) periods. NO_2^- nitrite, NO_3^- nitrate, and NH_4^+. (*) Not sampled.

During all the periods monitored, nitrate was the dominant fraction of DIN, representing up to 95% of the total DIN in both sectors. This indicates high levels of bacterial oxidation and nitrification within the estuary (Figures 7 and 8).

In the middle sector, where dissolved nutrient concentrations were 2 or 3 times higher than in the lower sector, trophic index scores were between 5.1 and 5.9, indicating a high level of eutrophication. This trophic status is reinforced by the remineralization of organic matter from the mangrove in the water column. While there was no alteration of the trophic status of this during the drought period, scores increased by up to 5.8, indicating high levels of eutrophication, probably due to the increase in the dissolved nutrient concentrations recorded in this period. Better conditions were observed in the lower sector, where scores of between 4.1 and 5.0 predominated, indicating moderate eutrophication. In this sector, high levels of eutrophication were observed only during periods with abnormally high rainfall, such as that observed during La Niña events, when dissolved nutrient concentrations increased (Figure 9).
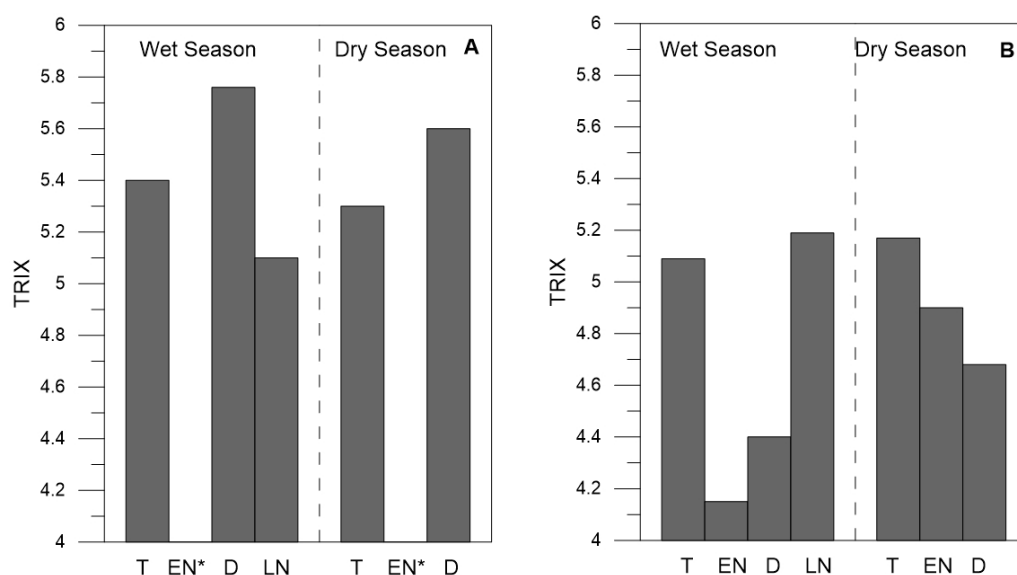

Figure 9. Trophic index recorded in the middle (**A**) and lower (**B**) sectors of the Caeté estuary in typical (T) and atypical (EN: El Niño, D: Drought, and LN: La Niña) periods. (*) Data are not available.

Chlorophyll *a* concentrations indicate that productivity was highest during the drought and El Niño events in the middle sector ($F = 1.41$; $p = 0.03$), where concentrations ranged mainly between 10 and 20 mg m^{-3}, indicating more productive waters. In the lower sector, values of less than 10 mg.m^{-3} indicated lower productivity than the middle sector, mainly during periods of decreased rainfall, such as El Niño events (Figure 10).

The Principal Components Analysis (PCA) of the middle sector (Figure 11A) indicated that the first axis, represented primarily by salinity, explained 27% of the total variance. A strong positive relationship was recorded with pH in the dry season, irrespective of the influence of climate events. Both salinity and pH are strongly influenced by marine conditions, which explains their strong correlation as well as their strong negative correlation with rainfall levels. The second axis, represented by dissolved oxygen concentrations, explained 20% of the total variance. This variable is related to turbidity. Both dissolved oxygen and turbidity increased during the rainy season in all years (typical and atypical), when increased turbulence contributed to more oxygenated waters and the resuspension of sediments in the water column.
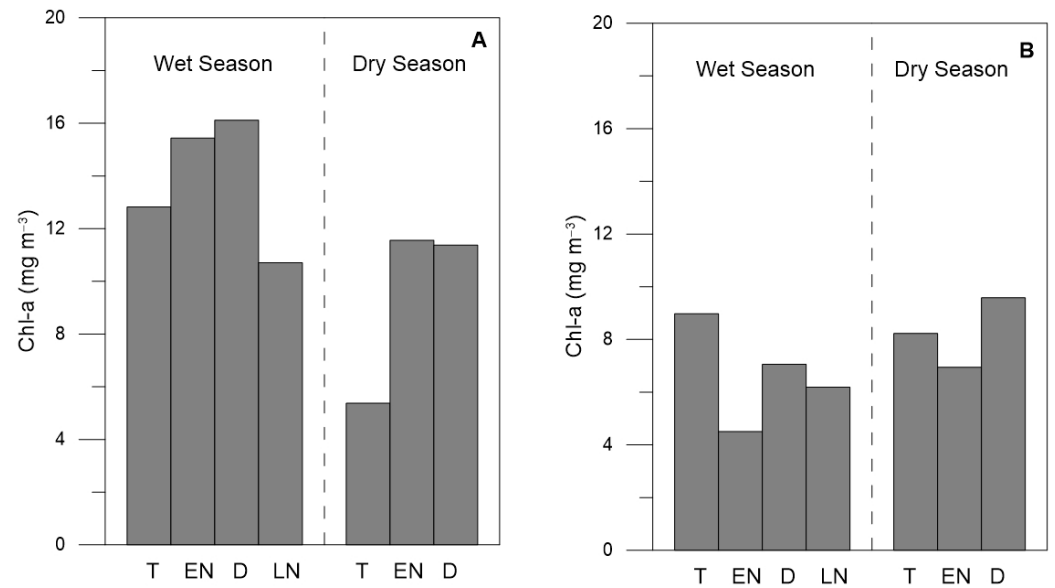
Figure 10. Chlorophyll *a* concentrations were recorded in the middle (**A**) and lower (**B**) sectors of the Caeté estuary during typical (T) and atypical (EN: El Niño, D: Drought, and LN: La Niña) periods.
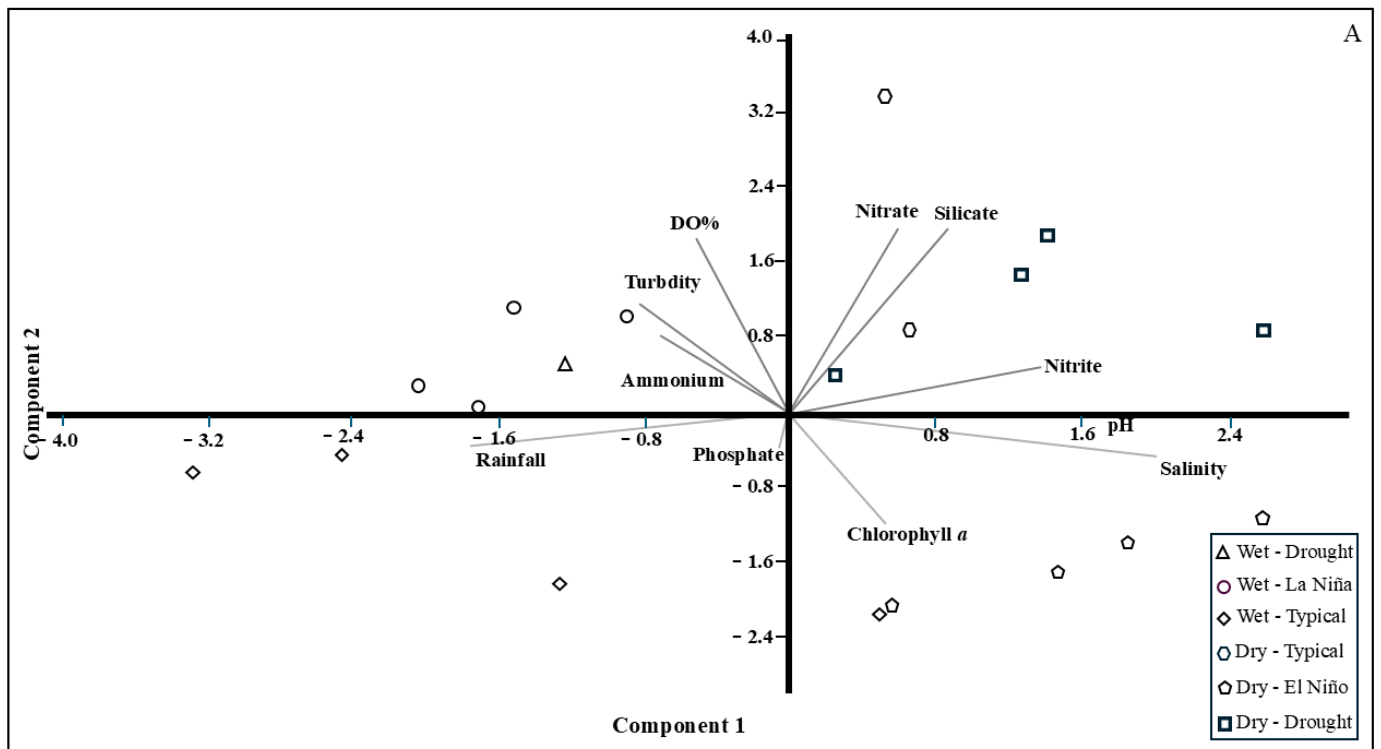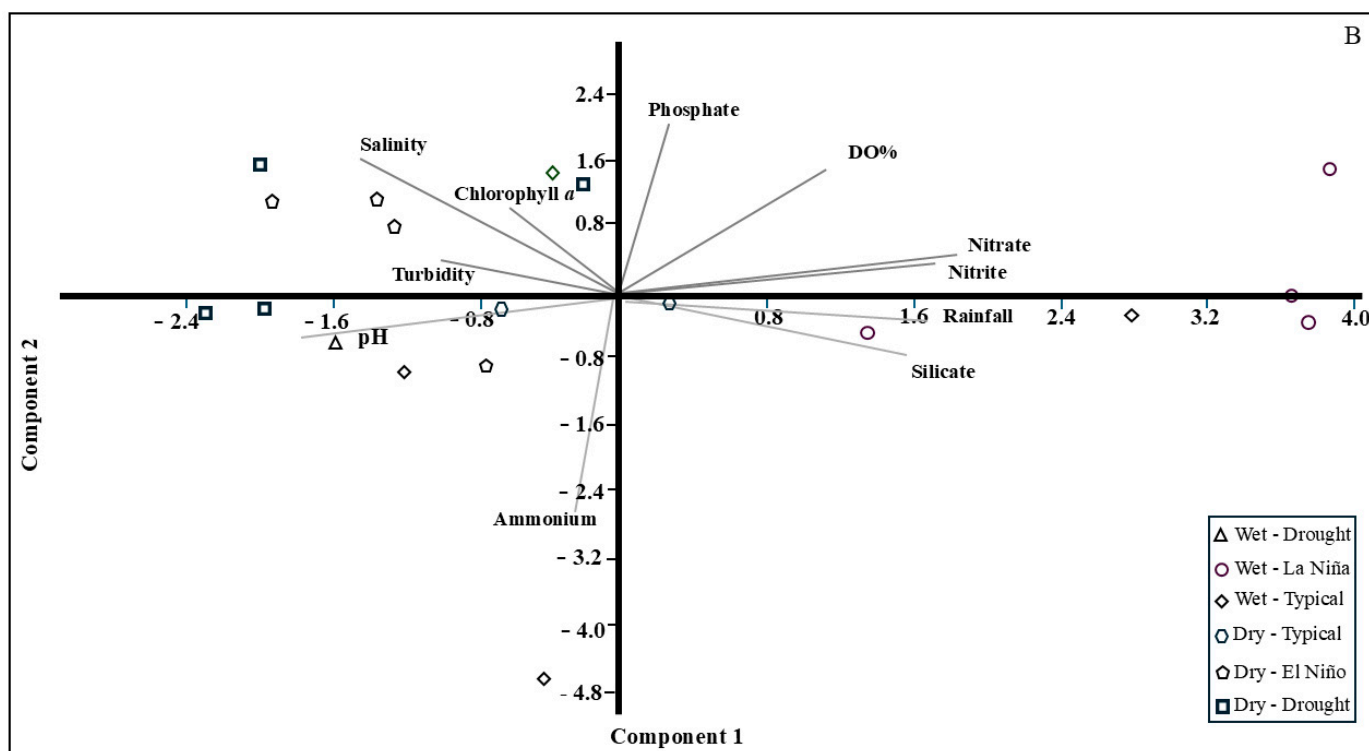

Figure 11. *Cont.*

Figure 11. Principal Components Analysis of rainfall and hydrological variables recorded in the middle (**A**) and lower (**B**) sectors of the Caeté estuary. Tip: Typical; EN: El Niño; D: Drought; LN: La Niña.

The PCA (Figure 11B) of the lower sector explained 57% of the total variance. The first axis explained 39% of the total variance, which was related to nitrate concentrations. This nutrient increased during La Niña events and was correlated strongly with other nutrients such as nitrite and silicate. This further reinforces the patterns outlined above, which indicate that the increase in freshwater discharge observed during La Niña events contributes to the transportation of dissolved nutrients to adjacent coastal waters. The second axis explained 18% of the variance and was represented mainly by ammonium, which presented the opposite pattern to the other parameters, presenting a stronger relationship with ortophosphate and other variables influenced by waters with a strong marine influence.

5. Discussion

5.1. Climatological Conditions

The Amazon region is marked by high annual rainfall rates, which may reach 3300 mm in the coastal zone during typical years [51]. During recent decades, a number of studies have shown that rainfall levels in the region have become increasingly variable due to the increase in the frequency and intensity of anomalous climate events [21]. For example, extreme rainfall levels and floods were recorded in 2008–2009 and 2015, alternating with strong droughts in 2005, 2007, 2010, 2013, and 2014. During some periods, in addition, while extreme levels of rainfall were recorded in the central Amazon region, drought conditions were experienced on the coast, as observed in 2012 [21,25,52].

Significant effects of extreme rainfall events or droughts have been detected in the Amazon coastal zone in some recent years. The El Niño event from August 2006 to February 2007 reduced rainfall levels in the Bragança region in 2007, and the rainy season started late, beginning only in February 2007. By contrast, the 2010 Amazon drought began in the early Austral summer, during an El Niño event, when the warming of the tropical North Atlantic resulted in an even more intense drought than that recorded in 2005, which had

been referred to as "the worst drought of the century" [21,23]. In 2010, the discharge of the Amazon River reached its lowest ever recorded level (8300 m^3 s^{-1}) during the austral spring [53]. During this event, rainfall decreased by 20% in the Bragança region, and river discharge was almost 40% lower than typical. Smaller deficits were recorded at other sites in the Amazon Coastal Zone, such as the city of Macapá, where river discharge decreased by around 10%, and Marajó Island, where it decreased by approximately 25% [54].

This drought was followed by an unprecedented increase in river discharge during the subsequent summer and autumn of 2011 [24]. The southward shift of the Intertropical Convergence Zone (ITCZ) coincided with negative SST anomalies in the central equatorial Pacific, producing La Niña-like conditions, which were responsible for the increase in rainfall levels. In the Caeté Estuary, as well as at Macapá and Marajó Island, rainfall increased by 5–15% in 2011 [54].

In 2012–2013, the Amazon coastal zone also appears to have been affected by a drought on the coast of northeastern Brazil, which began in 2012 [25]. This drought was caused by anomalously cold surface water in the subtropical South Atlantic. It induced an intensification of the high-pressure zone in the South Atlantic when the anomalously cold waters migrated to the north (10°–20° S), causing a northward displacement of the areas of high pressure. This high pressure interacted with sinking air masses induced by the strong upward motion in Amazonia, which determined the dry conditions in northeastern Brazil [25]. The effects of this phenomenon on rainfall levels were probably extended to the Amazon Coastal Zone, where a strong drought was observed.

The analysis of the long-term rainfall data for the Bragança region indicates that during drought or El Niño events, rainfall levels may be up to 45% lower than average. These anomalies are more pronounced during the rainy season, when rainfall typically exceeds 200 mm per quarter, as observed in 2007 (the rainy season started late). During La Niña events, by contrast, rainfall may be up to 60% higher than the mean. It is important to note that the relationship between extreme climate events and rainfall levels may vary considerably according to the frequency and intensity of the events.

5.2. Effects of Climate Events on Hydrological Aspects

The impacts of extreme climate events on the physical–chemical properties of the water in estuarine systems have been extensively reported around the world. In South America, an El Niño event contributed to an increase in the trophic status of the sediments of the Plate River Estuary due to an increase in freshwater input [5]. In the equatorial Nha Phu Estuary in southeast Vietnam, the strong La Niña of 2010 led to a reduction in salinity and an increase in primary production, probably fueled by the inflow of nutrient-rich freshwater [55].

In the estuaries of the Amazon region, studies documented oscillations in water quality linked systematically to the rainfall regime, which is in turn controlled by large-scale climatic phenomena [14,33,37,40,56,57]. The decrease in rainfall provoked by drought or El Niño conditions results in a decrease in freshwater discharge and a subsequent increase in the salinity of coastal waters. This increase in salinity is typically greater than that observed during a typical dry season. The opposite pattern has been observed under La Niña conditions at other sites on the Amazon coast, near the Caeté Estuary, including the Taperaçu Estuary [14] and Ajuruteua Beach [13], as well as macrotidal estuaries in Australia [9].

In the present study, however, the increase in rainfall associated with the La Niña event did not result in any clear decrease in salinity in the Caeté estuary. Probably, the accumulation of salt crystals in the mangrove during the previous months, marked by El Niño and drought events, resulted in the transfer of this salt to the estuary during the months of increased rainfall marked by the La Niña events of December 2010 and July 2011. A similar pattern was observed in this estuary during the rainy season in previous years [58,59].

The increase in dissolved inorganic nutrient concentrations in the middle sector of the estuary recorded during drought and El Niño events may be related to the retention of dissolved nutrients caused by the reduction in river discharge. As shown by [56], this tends to occur when rainfall levels decrease and mean freshwater discharge is lower than 45 m s^{-1}. This contributes to an increase in the trophic scores but is not enough to increase the trophic status of the estuary. During typical rainy seasons or La Niña events, by contrast, the high freshwater river discharge will induce the transport of dissolved inorganic nutrients to the lower sector. During the typical rainy season, tidal asymmetry increases, with a longer ebb tide (8 h) and higher ebb current displacement, up to 36 km [33], and during La Niña events, these conditions may be exacerbated, contributing to an increase in the trophic status of the estuary, as observed in the present study and in earlier studies in an area adjacent to the Caeté estuary under similar conditions [13].

In addition to their influence on dissolved nutrient concentrations and trophic status, extreme climate events may affect biological productivity in estuarine environments. This would account for the increased chlorophyll *a* concentrations (an indirect measure of biomass) observed in the middle sector of the Caeté estuary during drought and El Niño events [60]. The increase in salinity during these events may contribute to the desorption of phosphate from the bottom sediment, causing an increase in its concentrations in the water column [61]. This would favor the proliferation of diatoms, the second most abundant phytoplankton group in the Caeté estuary [62], which require compounds of phosphorus, silica, and nitrogen for their growth and the formation of their cell structure [63]. Other impacts of extreme climate events on biological productivity in estuaries have been reported in previous studies, such as those of [14,64,65].

Overall, the effects of extreme climate events in the Caeté estuary have contrasting characteristics. Negative rainfall anomalies caused by drought and El Niño events are responsible for high eutrophication in the middle sector but moderate eutrophication in the lower sector. Conversely, positive rainfall anomalies caused by La Niña events decrease the trophic scores in the middle sector of the estuary, although no changes in its trophic status were observed. At the same time, the trophic conditions of the lower sector increased. It is important to note that these effects will vary according to the intensity and duration of the climate events and that, in the Caeté estuary, the water presents eutrophic characteristics due to the natural input of dissolved nutrients from the extensive area of mangrove surrounding the estuary. Given this, the quality of the water in the Caeté estuary cannot be classified as poor, according to TRIX criteria.

6. Conclusions

During the climate events monitored in the present study, rainfall decreased by up to 92% in the months affected by drought or El Niño conditions and increased between 15% and 100% in the months affected by La Niña conditions. These processes affected freshwater discharge into the estuary, altering the potential of this variable for the regulation of water quality.

As observed here, drought or El Niño events contribute to a significant decrease in rainfall levels, with the water in the estuary becoming more saline and alkaline and less oxygenated in both the middle and lower sectors. During these events, high concentrations of dissolved nutrients and eutrophic conditions are typically found in the middle sector of the estuary. During La Niña events, the dissolved nutrient concentrations decrease, but the trophic status of the estuary is unaltered. The lower sector presented a distinct pattern, with lower dissolved nutrient concentrations, moderate eutrophication of the water during El Niño and drought events, and high eutrophication during La Niña events. Fluctuations in the frequency and intensity of climate events may thus minimize or exacerbate the trophic status of the Caeté estuary.

As few data are available on the effects of extreme climate events in Amazonian coastal environments, these findings can be considered to be an important work of reference for

the assessment of the effects of these events on other natural environments in the Amazon coastal zone.

7. Further Research Questions

During this study, several challenges were identified for improving or expanding the database established for the Caeté estuary. These include (i) applying more detailed procedures for calculating nutrient input into the Caeté estuary; (ii) continuing to monitor hydrological variables to provide a reliable time series for establishing an appropriate trophic index for the Amazon region; and (iii) including biotic variables, such as fecal coliforms, which have been shown to be good indicators of water quality. Once the first empirical knowledge about the functioning of the Caeté estuary is provided, the application of a numerical modeling approach to predict the microbiological and trophic state of the Caeté estuary is necessary, considering the different conditions of rainfall and river discharge, tidal heights, and current dynamics.

Author Contributions: Conceptualization, M.C.M. and L.C.C.P.; methodology, M.C.M. and L.C.C.P.; validation, M.C.M., L.C.C.P. and R.M.d.C.; formal analysis, L.C.C.P.; investigation, M.C.M. and L.C.C.P.; resources, M.C.M., L.C.C.P. and R.M.d.C.; data curation, M.C.M. and L.C.C.P.; writing—original draft preparation, M.C.M. and L.C.C.P.; writing—review and editing, M.C.M., L.C.C.P. and R.M.d.C.; visualization, M.C.M. and L.C.C.P.; supervision, L.C.C.P.; project administration, L.C.C.P.; funding acquisition, M.C.M., L.C.C.P. and R.M.d.C. All authors have read and agreed to the published version of the manuscript.

Data Availability Statement: Data will be available on request.

Conflicts of Interest: The authors declare no conflict of interest.

References

1. Kennish, M.J. Environmental threats and environmental future of estuaries. *Environ. Conserv.* **2002**, *29*, 78–107. [CrossRef]
2. Whittaker, R.H.; Likens, G.E. The biosphere and man. In *Primary Productivity of the Biosphere*; Lieth, H., Whittaker, R.H., Eds.; Springer: New York, NY, USA, 1975; pp. 305–328.
3. McLusky, D.S.; Elliott, M. *The Estuarine Ecosystem: Ecology, Threats and Management*; Oxford University Press: New York, NY, USA, 2004. [CrossRef]
4. Elliott, M.; Quintino, V. The Estuarine Quality Paradox, Environmental Homeostasis and the difficulty of detecting anthropogenic stress in naturally stressed areas. *Mar. Pollut. Bull.* **2007**, *54*, 640–645. [CrossRef] [PubMed]
5. García-Rodríguez, F.; Brugnoli, E.; Muniz, P.; Venturini, N.; Burone, L.; Hutton, M.; Rodriguez, M.; Pita, A.; Kandratavicius, N.; Perez, L.; et al. Warm-phase ENSO events modulate the continental freshwater input and the trophic state of sediments in a large South American estuary. *Mar. Freshw. Res.* **2013**, *65*, 1. [CrossRef]
6. Pereira, L.C.C.; Costa, A.K.R.; Costa, R.M.; Magalhães, A.; Flores-Montes, M.J.; Jiménez, J.A. Influence of a drought event on hydrological characteristics of a small estuary on the amazon mangrove coast. *Estuaries Coasts* **2017**, *41*, 676–689. [CrossRef]
7. Woodward, G.; Bonada, N.; Brown, L.E.; Death, R.G.; Durance, I.; Gray, C.; Hladyz, S.; Ledger, M.E.; Milner, A.M.; Ormerod, S.J.; et al. The effects of climatic fluctuations and extreme events on running water ecosystems. *Philos. Trans. R. Soc.* **2016**, *371*, 20150274. [CrossRef]
8. Wetz, M.S.; Yoskowitz, D.W. An 'extreme' future for estuaries? Effects of extreme climatic events on estuarine water quality and ecology. *Mar. Pollut. Bull.* **2013**, *69*, 7–18. [CrossRef]
9. Thompson, P.A.; O'Brien, T.D.; Paerl, H.W.; Peierls, B.L.; Harrison, P.J.; Robb, M. Precipitation as a driver of phytoplankton ecology in coastal Waters: A climatic perspective. *Estuar. Coast. Shelf Sci.* **2015**, *162*, 119–129. [CrossRef]

10. Costa, A.K.R.; Pereira, L.C.C.; Jiménez, J.A.; Oliveira, A.R.G.; Flores-Montes, M.J.; Costa, R.M. Effects of Extreme Climatic Events on the Hydrological Parameters of the Estuarine Waters of the Amazon Coast. *Estuaries Coasts* **2022**, *45*, 1517–1533. [CrossRef]

11. Oliveira, A.R.G.; Queiroz, J.B.M.; Pardal, E.C.; Pereira, L.C.C.; Costa, R.M. How does the phytoplankton community respond to the effects of La Niña and post-drought events in a tide-dominated Amazon estuary? *Aquat. Sci.* **2023**, *85*, 9. [CrossRef]

12. Procópio, A.D.; Costa, R.M.; Magalhães, A.; Silva, D.C.; Silva, T.R.C.; Fernandes, F.S.; Pereira, L.C.C. Effects of the El Niño 2015/2016 event on Acartia tonsa and A. lilljeborgii (Copepoda) production in a Brazilian Amazon estuary. *Ecohydrol. Hydrobiol.* 2024, *in press*. [CrossRef]

13. Pereira, L.C.C.; Oliveira, S.M.O.; Costa, R.M.; Costa, K.G.; Vila-Concejo, A. What happens on na equatorial beach on the Amazon coast when La Niña occurs during the rainy season? *Estuar. Coast. Shelf Sci.* **2013**, *135*, 116–127. [CrossRef]

14. Andrade, M.P.; Magalhães, A.; Pereira, L.C.C.; Flores-Montes, M.J.; Pardal, E.C.; Andrade, T.P.; Costa, R.M. Effects of a La Niña evento n hydrological patterns and copepod community structure in a shallow tropical estuary (Taperaçu, Northern Brazil). *J. Mar. Syst.* **2016**, *164*, 128–143. [CrossRef]

15. Figueroa, S.N.; Nobre, C. Precipitation distribution over Central and Western Tropical South America. *Climanálise* **1990**, *5*, 36–45.

16. Fernandes, K.; Baethgen, W.; Bernardes, S.; DeFries, R.; DeWitt, D.G.; Goddard, L.; Lavado, W.; Lee, D.E.; Padoch, C.; Pinedo-Vasquez, M.; et al. North Tropical Atlantic influence on western Amazon fire season variability. *Geophys. Res. Lett.* **2011**, *38*, L12701. [CrossRef]

17. García-García, D.; Ummenhofer, C.C. Multidecadal variability of the continental precipitation annual amplitude driven by AMO and ENSO. *Geophys. Res. Lett.* **2015**, *42*, 526–535. [CrossRef]

18. Marengo, J.A.; Nobre, C.A.; Oyama, T.M.; Sampaio, G.; Camargo, H.; Alves, L.; Oliveira, R. The Drought of Amazonia in 2005. *J. Clim.* **2008**, *21*, 495–516. [CrossRef]

19. Zeng, N.; Yoon, J.; Marengo, J.A.; Subramanian, A.; Nobre, C.A.; Mariotti, A.; Neelin, J.D. Causes and impacts of the 2005 Amazon drought. *Environ. Res. Lett.* **2008**, *3*, 014002. [CrossRef]

20. Yoon, J.H.; Zeng, N. An Atlantic influence on Amazon rainfall. *Clim. Dyn.* **2010**, *34*, 249–264. [CrossRef]

21. Coelho, C.A.S.; Cavalcanti, I.A.F.; Costa, S.M.S.; Freitas, S.R.; Ito, E.R.; Luz, G.; Santos, A.F.; Nobre, C.A.; Marengo, J.A.; Pezza, A.B. Climate diagnostics of three major drought events in the Amazon and illustrations of their seasonal precipitation predictions. *Meteorol. Appl.* **2012**, *19*, 237–255. [CrossRef]

22. Trenberth, K.E.; Dai, A.; Van Der Schrier, G.; Jones, P.D.; Barichivich, J.; Briffa, K.R.; Sheffield, J. Global warming and changes in drought. *Nat. Clim. Chang.* **2014**, *4*, 17–22. [CrossRef]

23. Marengo, J.A.; Tomasella, J.; Alves, L.M.; Soares, W.R.; Rodriguez, D.A. The drought of 2010 in the Amazon region. *Geophys. Res. Lett.* **2011**, *38*, L12703.

24. Espinoza, J.C.; Ronchail, J.; Guyot, J.L.; Junquas, C.; Drapeau, G.; Martinez, J.M.; Santini, W.; Vauchel, P.; Lavado, W.; Ordoñez, J.; et al. From drought to flooding: Understanding the abrupt 2010–11 hydrological anual cycle in the Amazonas River and tributaries. *Environ. Res. Lett.* **2012**, *7*, 024008. [CrossRef]

25. Marengo, J.A.; Borma, L.S.; Rodriguez, D.A.; Pinho, P.; Soares, W.R.; Alves, L.M. Recent extremes of drought and flooding in Amazonia: Vulnerabilities and human adaptation. *Am. J. Clim. Chang.* **2013**, *2*, 87–96. [CrossRef]

26. Williams, E.; Dall' Antonia, A.; Dall' Antonia, V.; Almeida, J.M.; Suarez, F.; Liebmann, B.; Malhado, C.M. The drought of the century in the Amazon Basin: An analysis of the regional variation of rainfall in South America in 1926. *Acta Amaz.* **2005**, *35*, 231–238. [CrossRef]

27. Xu, L.; Samantha, A.; Costa, M.H.; Ganguly, S.; Nemani, R.R.; Myneni, R.B. Widespread decline in greenness of Amazonian vegetation due to the 2010 drought. *Geophys. Res. Lett.* **2011**, *38*, L07402. [CrossRef]

28. Pinho, P.F.; Orlove, B.; Lubell, M. Overcoming barriers to collective action in community-based fisheries management in the Amazon. *Hum. Organ.* **2012**, *71*, 99–109. [CrossRef]

29. Seneviratne, S.I.; Nicholls, N.; Easterling, D.; Goodess, C.M.; Kanae, S.; Kossin, J.; Luo, Y.; Marengo, J.; Mcinnes, K.; Rahimi, M.; et al. Changes in climate extremes and their impacts on the natural physical environment. In *Managing the Risks of Extreme Events and Disasters to Advance Climate Change Adaptation*; Field, C.B., Barros, V., Stocker, T.F., Qin, D., Dokken, D.J., Ebi, K.L., Mastrandrea, M.D., Mach, K.J., Plattner, G.K., Allen, S.K., et al., Eds.; Cambridge University Press: Cambridge, UK, 2012; pp. 109–230.

30. Tomasella, J.; Pinho, P.F.; Borma, L.S.; Marengo, J.A.; Nobre, C.A.; Bittencourt, O.R.F.O.; Prado, M.C.R.; Rodriguez, D.A.; Cuartas, L.A. The droughts of 1997 and 2005 in Amazonia: Floodplain hydrology and its potential ecological and human impacts. *Clim. Chang.* **2013**, *116*, 723–746. [CrossRef]

31. Marengo, J.A.; Alves, L.M.; Wagner, R.S.; Rodriguez, D.A. Two Contrasting Severe Seasonal Extremes in Tropical South America in 2012: Flood in Amazonia and Drought in Northeast Brazil. *Am. Meteorol. Soc.* **2013**, *26*, 9137–9154. [CrossRef]

32. Dittmar, T.; Lara, R.J. Driving forces behind nutrient and organic matter dynamics in a mangrove tidal creek in North Brazil.Estuarine. *Coast. Shelf Sci.* **2001**, *52*, 249–259. [CrossRef]

33. Monteiro, M.C.; Jiménez, J.A.; Pereira, L.C.C. Natural and human controls of water quality of na Amazon estuary (Caeté-PA, Brazil). *Ocean Coast. Manag.* **2016**, *124*, 42–52. [CrossRef]

34. Wolf, M.; Koch, V.; Isaac, V. A Trophic flow model of the Caeté mangrove estuary (North Brazil) with considerations for the sustainable use of its resources. *Estuar. Coast. Shelf Sci.* **2000**, *50*, 789–803. [CrossRef]

35. Krause, G.; Schories, D.; Glaser, M.; Diele, K. Spatial Patterns of Mangrove Ecosystems: The Bragantinian Mangroves of Northern Brazil (Bragança, Pará). *Ecotropica* **2001**, *7*, 93–107.

36. Lara, R.J.; Dittmar, T. Nutrient dynamics in a mangrove creek (North Brazil) during the dry season. *Mangroves Salt Marshes* **1999**, *3*, 185–195. [CrossRef]

37. Monteiro, M.C.; Pereira, L.C.C.; Jiménez, J.A. The trophic status of an amazonian estuary under anthropogenic pressure (Brazil). *J. Coast. Res. SI* **2016**, *75*, 98–102. [CrossRef]

38. IBGE—Instituto Brasileiro de Geografia e Estatística. Estimativas da População de. 2015. Available online: http://www.ibge.gov.br/home/estatistica/populacao/estimativa2015 (accessed on 16 March 2016).

39. Guimarães, D.O.; Pereira, L.C.C.; Costa, R.M. Aspectos Socioeconômicos e Ambientais das Comunidades Rurais da Bacia Hidrográfica do Rio Caeté (Pará-Brasil). *Gerenciamento Costeiro Integr.* **2009**, *9*, 71–84. [CrossRef]

40. Pereira, L.C.C.; Monteiro, M.C.; Guimarães, D.O.; Costa, R.M. Seasonal effects of wastewater to the water quality of the Caeté river estuary. *An. Acad. Bras. Ciênc.* **2010**, *82*, 467–478. [CrossRef]

41. Sousa, N.S.S.; Monteiro, M.C.; Gorayeb, A.; Costa, R.; Pereira, L.C.C. Effects of sewage on natural enrironments of the amazona region (Pará-Brazil). *J. Coast. Res. SI* **2016**, *75*, 158–162. [CrossRef]

42. NOAA—National Oceanic and Atmospheric Administration. Climate Prediction Center. 2018. Available online: www.cpc.ncep.noaa.gov/products/precip/CWlink/MJO/enso.shtml (accessed on 20 May 2018).

43. Marengo, J.A.; Espinoza, J.C. Extreme seasonal droughts and floods in Amazonia: Causes, trends and impacts. *Int. J. Climatol.* **2015**, *36*, 1033–1050. [CrossRef]

44. Parsons, T.R.; Strickland, J.D.H. Discusson of spectrophometric determination of marine-plant pigments, with revised equations for ascertaining chlorophyll a and carotenois. *J. Mar. Res.* **1963**, *21*, 105–156.

45. UNESCO—United Nations Educational, Scientific and Cultural Organization. *Determination of Photosynthetic Pigments in Sea-Water*; UNESCO: Paris, France, 1966.

46. Strickland, J.D.H.; Parsons, T.R.A. *A Practical Handbook of Seawater Analysis*; Bulletin 167; Alger Press: Ottawa, ON, Canada, 1972.

47. Grasshoff, K.; Emrhardt, M.; Kremling, K. *Methods of Seawater Analysis*; Verlag Chemie: New York, NY, USA, 1983.

48. Vollenweider, R.A.; Giovanardi, F.; Rinaldi, A. Characterization of the trophic conditions of marine coastal waters with special reference to the NW Adriatic Sea: Proposal for a trophic scale, turbidity and generalized water quality index. *Environmetrics* **1998**, *9*, 329–357. [CrossRef]

49. Conover, W.O.J. *Pratical Nonparametric Statistics*; Jonh Wiley: New York, NY, USA, 1971.

50. Sokal, R.R.; Rohlf, F.J. *Biometry: The Principles and Pratice of Numerical Classification in Biological Research*; W.H. Freeman: San Francisco, CA, USA, 1969.

51. CPTEC/INMET. *Climatologia de Precipitação (mm) 2018*; CPTEC/INMET: PARÁ, Brazil, 2018.

52. Gloor, M.; Brienen, R.J.W.; Galbraith, D.; Feldpausch, T.R.; Schöngart, J.; Guyot, J.L.; Espinoza, J.C.; Lloyd, J.; Phillips, O.L. Intensification of the Amazon hydrological cycle over the last two decades. *Geophys. Res. Lett.* **2013**, *40*, 1729–1733. [CrossRef]

53. Espinoza, J.C.; Lengaigne, M.; Ronchail, J.; Janicot, S. Large-scale circulation patterns and related rainfall in the Amazon Basin: A neuronal networks approach. *Clim. Dyn.* **2012**, *38*, 121–140. [CrossRef]

54. INMET (Instituto Nacional de Meteorologia). 2018. Available online: http://www.inmet.gov.br/portal/index.php?r=estacoes/estacoesconvencionais (accessed on 14 April 2020).

55. Lund-Hansen, L.C.; Thorbjørn, K.T.; Andersen, J.; Nielsen, M.H.; Doan-Nhu, H.; Nguyen-Ngoc, L. Impacts and effects of a historical high and ENSO linked freshwater inflow in the tropical estuary Nha Phu, southeast Vietnam. *Reg. Stud. Mar. Sci.* **2018**, *17*, 28–37. [CrossRef]

56. Costa, A.K.R.; Pereira, L.C.C.; da Costa, R.M.; Monteiro, M.C.; Flores-Montes, M.J. Oceanographic processes in an Amazon estuary during an atypical wet season. *J. Coast. Res. SI* **2013**, *65*, 1104–1109. [CrossRef]

57. Monteiro, M.C.; Pereira, L.C.C.; Guimarães, D.O.; Costa, R.M.; Souza-Filho, P.W.M.; Vieira, S.R.; Jiménez, J.A. Influence of natural and anthropogenic conditions on the water quality of the Caeté River Estuary (NE Brazil). *J. Coast. Res. SI* **2011**, *64*, 1535–1539.

58. Cohen, M.C.L.; Lara, R.J. Temporal changes of mangrove vegetation boundaries in Amazonia: Application of GIS and remote sensing techniques. *Wetl. Ecol. Manag.* **2003**, *11*, 223–231. [CrossRef]

59. Magalhães, A.; Costa, R.M.; Liang, T.H.; Pereira, L.C.C.; Ribeiro, M.J.S. Spatial and temporal distribution in density and biomass of two Pseudodiaptomus species (Copepoda: Calanoida) in the Caeté River Estuary (Amazon region-North of Brazil). *Braz. J. Biol.* **2006**, *66*, 421–430. [CrossRef]

60. Pereira, L.C.C.; Jiménez, J.A.; Pineda, M.G.; Costa, A.K.R.; Sousa, N.S.S.; Oliveira, A.R.G.; Costa, R.M. Assessment of trophic status in Amazonian estuaries: A reinterpretation of TRIX values in mangrove estuaries. *Ocean Coast. Manag.* **2023**, *244*, 106805. [CrossRef]

61. Pereira, L.C.C.; Sousa, N.S.S.; Rodrigues, L.M.S.; Monteiro, M.C.; Silva, S.R.S.; Oliveira, A.R.G.; Dias, A.B.B.; Costa, R.M. Effects of the lack of basic public sanitation on the water quality of the Caeté River estuary in northern Brazil. *Ecohydrol. Hydrobiol.* **2021**, *21*, 299–314. [CrossRef]

62. Matos, J.B.; Sodré, D.K.L.; Costa, K.G.; Pereira, L.C.C.; Costa, R.M. Spatial and temporal variation in the composition and biomass of phytoplankton in an Amazonian estuary. *J. Coast. Res. SI* **2011**, *64*, 1525–1529.

63. Hildebrand, M. Diatoms, Biomineralization Processes, and Genomics. *Chem. Rev.* **2008**, *108*, 4855–4874. [CrossRef] [PubMed]

64. Sathicq, M.B.; Bauer, D.E.; Gómez, N. Influence of El Niño Southern Oscillation phenomenon on coastal phytoplankton in a mixohaline ecosystem on the southeastern of South America: Río de la Plata estuary. *Mar. Pollut. Bull.* **2015**, *98*, 26–33. [CrossRef] [PubMed]

65. Zhang, Z.; Craft, C.B.; Xue, Z.; Tong, S.; Lu, X. Regulating effects of climate, net primary productivity, and nitrogen on carbon sequestration rates in temperate wetlands, Northeast China. *Ecol. Indic.* **2016**, *70*, 114–124. [CrossRef]